

# Collective Chaos Induced by Structures of Complex Networks

Huijie Yang<sup>a,\*</sup>, Fangcui Zhao<sup>b</sup> and Binghong Wang<sup>a</sup>

<sup>a</sup>*Department of Modern Physics, University of Science and Technology of China, Hefei Anhui 230026, China*

<sup>b</sup>*College of Life Science and Biomedical Engineering, Beijing University of Technology, Beijing 100022, China*

---

## Abstract

Mapping a complex network of  $N$  coupled identical oscillators to a quantum system, the nearest neighbor level spacing (NNLS) distribution is used to identify collective chaos in the corresponding classical dynamics on the complex network. The classical dynamics on an Erdos-Renyi network with the wiring probability  $p_{ER} \leq \frac{1}{N}$  is in the state of collective order, while that on an Erdos-Renyi network with  $p_{ER} > \frac{1}{N}$  is in the state of collective chaos. The dynamics on a WS Small-world complex network evolves from collective order to collective chaos rapidly in the region of the rewiring probability  $p_r \in [0.0, 0.1]$ , and then keeps chaotic up to  $p_r = 1.0$ . The dynamics on a Growing Random Network (GRN) is in a special state deviates from order significantly in a way opposite to that on WS small-world networks. Each network can be measured by a couple values of two parameters  $(\beta, \eta)$ .

*Key words:* Complex networks, Collective chaos, Spectra statistics

*PACS:* 05.50.+q, 05.10.-a, 05.40.-a, 87.18.Sn

---

## 1 Introduction

Impacts of network structures on the dynamical processes attract special attentions in recent years, to cite examples, the epidemic spreading on networks [1-3], the response of complex networks to stimuli [4,5] and the synchronization of dynamical systems on networks [6-9]. In this paper, we will consider the collective motions on complex networks, just like the phonon in regular lattices.

---

\* Corresponding author. E-mail: huijieyangn@eyou.com

By means of the random matrix theory (RMT), we find that the nearest neighbor level spacing (NNLS) distributions for spectra of complex networks generated with WS Small-world, Erdos-Renyi and Growing Randomly Network models can be described with Brody distribution in a unified way. This unified description can be used as a new measurement to characterize complex networks. The results tell us that the topological structure of a complex network can induce a special kind of collective motions. Under environmental perturbations, the collective motion modes can transition between each other abruptly. This kind of sensitivity to outside perturbations is called collective chaos in this paper. It is found that the properties of the collective chaos are determined only by the structures of the networks. Without the aid of the dynamical model presented in references [4,5], we show for the first time that the dynamics on complex networks can be in collective order, soft chaotic or even hard chaotic states.

## 2 The Method

Wigner, Dyson, Mehta and others developed the Random Matrix Theory (RMT) to understand the energy levels of complex nuclei and other kinds of complex quantum systems [10-13]. In recent literature, the spectral density function and the time series analysis methods are used to capture properties of complex networks [14-19]. One of the most important concepts in RMT is the nearest neighbor level spacing (NNLS) distribution. A general picture emerging from experiments and theories is that if the classical motion of a dynamical system is regular, the NNLS distribution of the corresponding quantum system behaves according to a Poisson distribution. If the corresponding classical motion is chaotic, the NNLS distribution will behave in accordance with the Wigner-Dyson ensembles. This is the content of the famous Bohigas conjecture [20,21]. Hence, the NNLS distribution of a quantum system can tell us the dynamical properties of the corresponding classical system.

Consider an undirected network of  $N$  coupled identical oscillators. The Hamiltonian reads,

$$H = \sum_{n=1}^N h_0(x_n, p_n) + \frac{1}{2} \cdot \sum_{m \neq n}^N A_{mn} \cdot V(x_m, x_n), \quad (1)$$

where,  $h_0(x_n, p_n)$  is the Hamiltonian of the  $n$ 'th oscillator,  $V(x_m, x_n)$  the coupling potential between the  $m$ 'th and the  $n$ 'th oscillators and  $A$  the adjacent matrix of the network. The Hamiltonian of the corresponding quantum system

can be represented as,

$$\hat{H} = \sum_{n=1}^N \hat{h}_0(x_n, p_n) + \frac{1}{2} \cdot \sum_{m \neq n}^N A_{mn} \cdot \hat{V}(x_m, x_n) \quad . \quad (2)$$

Assuming the site energy of each oscillator is  $\varepsilon_0$  and the eigenfunction is  $\varphi_0$ , we have  $\hat{h}_0(x_n, p_n)\varphi_0(x_n) = \varepsilon_0\varphi_0(x_n)$ . The matrix elements of  $\hat{H}$  reads,

$$\begin{aligned} H_{mn} &= \langle \varphi_0(x_m) | h_0(x_m) | \varphi_0(x_n) \rangle + A_{mn} \cdot \langle \varphi_0(x_m) | V(x_m, x_n) | \varphi_0(x_n) \rangle \\ &= \varepsilon_0 \cdot \delta_{mn} + A_{mn} \cdot V_{mn} \end{aligned} \quad (3)$$

The pattern of the spectrum of  $\hat{H}$  does not dependent on the values of  $\varepsilon_0$  and  $V_{mn}$ . Assigning  $\varepsilon_0 = 0$  and  $V_{mn} = 1$ , we have  $H = A$ . By this way, the spectrum of the adjacent matrix  $A$  can be used to calculate the NNLS distribution of the quantum system. To make our discussion as self-contained as possible, we review briefly the procedure to obtain the NNLS distribution from the spectrum of  $A$ , denoted with  $\{E_i | i = 1, 2, 3, \dots, N\}$ .  $N$  is the total number of the energy levels.

To ensure that the distances between the energy levels are expressed in units of local mean energy level spacing, we should first map the energy levels  $E_i$  to new variables called “unfolded energy levels”  $\xi_i$ . This procedure is called unfolding, which is generally a non-trivial task [22].

Define the cumulative density function as,

$$G(E) \equiv N \int_{-\infty}^E g(s) ds, \quad (4)$$

where  $g(s)$  is the density function of the initial energy level spectrum. We have,

$$G(E) | E_{k+1} > E \geq E_k = k. \quad (5)$$

Preprocess the spectrum,  $\{E_k | k = 1, 2, 3, \dots, N\}$ , and the corresponding accumulative density function,  $\{G(E_k) | k = 1, 2, 3, \dots, N\}$ , so that for each of

them the mean is set to zero and the variance equals to 1, i.e.,

$$\lambda_k = \frac{E_k - \frac{1}{N} \sum_{m=1}^N E_m}{\left[ \sum_{j=1}^N \left( E_j - \frac{1}{N} \sum_{m=1}^N E_m \right)^2 \right]^{1/2}}, \quad (6)$$

$$F(\lambda_k) = \frac{G(E_k) - \frac{1}{N} \sum_{m=1}^N G(E_m)}{\left[ \sum_{j=1}^N \left( G(E_j) - \frac{1}{N} \sum_{m=1}^N G(E_m) \right)^2 \right]^{1/2}}. \quad (7)$$

Dividing the accumulative function  $F(\lambda)$  into two components, i.e., the smooth term  $F_{av}(\lambda)$  and the fluctuation term  $F_f(\lambda)$ , the unfolded energy levels can be obtained as,

$$\xi_k = F_{av}(\lambda_k). \quad (8)$$

Because we have not enough information on the accumulative density function at present time, a polynomial is employed to describe the relation between  $\xi_k$  and  $\lambda_k$ , as follows,

$$\xi_k = \sum_{l=0}^L c_l \cdot (\lambda_k)^l = F_{av}(\lambda_k). \quad (9)$$

It is found that a large value of  $L > 9$  can lead to a considerable good fitting result. To guarantee the fitting results exact enough, we assign the value as  $L = 17$ .

Defining the nearest neighbor level spacing (NNLS) as,

$$\left\{ s_i = w \cdot \frac{(\xi_{i+1} - \xi_i)}{\sigma_\xi} \right\} | i = 1, 2, 3, \dots (N-1), \quad (10)$$

the Brody distribution of the NNLS reads,

$$P(s) = \frac{\beta}{\eta} s^{\beta-1} \exp \left[ - \left( \frac{s}{\eta} \right)^\beta \right], \quad (11)$$

which is also called Weibull distribution in the research field of life data analysis [23]. In the definition of NNLS,  $w$  is a factor to make the values of the NNLS in a conventional range to get a reliable fitting result, and  $\sigma_\xi = \sqrt{\frac{\sum_{i=1}^{N-1} \xi_i^2}{N-1}}$ . In-

roducing the function,  $Q(s) = \int_0^s P(t)dt$ , some trivial computation lead to [23],

$$\ln R(s) \equiv \ln \left[ \ln \left( \frac{1}{1 - Q(s)} \right) \right] = \beta \ln s - \beta \ln \eta, \quad (12)$$

based upon which we can get reliable values of the parameters  $\beta$  and  $\eta$ .

To obtain the function  $Q(s)$ , we should divide the interval where the NNLS distributes into many bins. The size of a bin can be chosen to be a fraction of the square root of the variance of the NNLS, which reads,  $\varepsilon = \frac{1}{R} \sqrt{\frac{\sum_{i=1}^{N-1} s_i^2}{N-1}}$ . If  $R$  is unreasonable small,  $Q(s)$  cannot capture the exact features in actual probability distribution function (PDF), while a much large  $R$  will induce strong fluctuations. The value of the parameter  $R$  is assigned 20 in this paper, because the fitting results are stable in a considerable wide range about this value.

A Brody distribution reveals that the corresponding classical complex system is in a soft chaotic state [10]. For the two extreme conditions of  $\beta = 1$  and  $\beta = 2$ , the Brody distribution will reduce to the Poisson and the Wigner distributions. And the corresponding classical complex systems are in the hard chaotic and order states, respectively.

For the quantum system considered in this paper, it can be initially in a quantum state of  $|E_n\rangle$ , corresponding to the eigenvalue of  $E_n$ . Under a weak environmental perturbation, the state will display completely different behaviors [24-26]. If the system is in an order state, the transition probability of the initial state to a new state  $|E_m\rangle$  will decrease rapidly with the increase of  $|E_n - E_m|$ , and the transition occurs mainly between the initial state and its neighboring states. If the system is in a chaotic state, the transitions between all the states in the chaotic regime the initial state belongs to can occur with almost same probabilities. In the classical dynamics, the corresponding states are the collective motion modes, just like phonon in regular lattices. Under perturbations the state of a chaotic system can transition between the collective modes in the same chaotic regime abruptly, while the state of an order system can transition between the initial mode and its neighboring states only. Consequently, the chaotic state of the  $N$  identical oscillators is a kind of collective behavior rather than the individual properties of each oscillator. It is called collective chaos in this paper. The above discussions tell us that this collective chaos depends only on the structure of the undirected network.

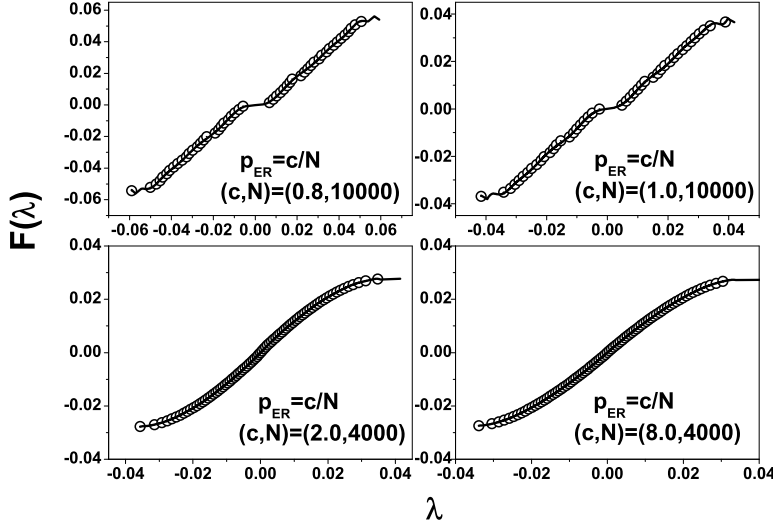


Fig. 1. The cumulative density function of the spectra of four Erdos-Renyi networks. The circles are the actual values, while the solid lines are fitting results with a 17-ordered polynomial function.

### 3 Results

Given  $N$  nodes, an Erdos-Renyi network can be constructed just by connecting each pair with a probability  $p_{ER}$  [27,28]. It is demonstrated that there exists a critical point  $p_c = \frac{1}{N}$ . For  $p_{ER} < p_c$ , the adjacency matrix can reduce into many sub-matrices, the couplings between the energy levels will be very weak and the NNLS will obey a Poisson form. For  $p_{ER} \geq p_c$ , the fraction of the nodes forming the largest sub-graph grows rapidly. The couplings between the energy levels will become stronger and stronger, and the NNLS should obey a Brody or even a Wigner form. Simulation results presented in Fig.1 to Fig.3 are consistent with this theoretical prediction.

Secondly, we consider the one-dimensional lattice small-world model designed by Watts and Strogatz (WS small-world model) [29]. Take a one-dimensional lattice of nodes with periodic boundary conditions, and join each node with its  $k$  right-handed nearest neighbors. Going through each edge in turn and with probability  $p_r$  rewiring one end of this edge to a new node chosen randomly. During the rewiring procedure double edges and self-edges are forbidden. Numerical simulations by Watts and Strogatz show that this rewiring process allows the small-world model to interpolate between a regular lattice and a random graph with the constraint that the minimum degree of each node is fixed [29]. The parameter  $k$  is chosen to be 2, and  $N$  is 3000. Fig.4 to Fig.6 present some typical results for different values of rewiring probability. In the main region we are interested, the NNLS distribution can be described with a

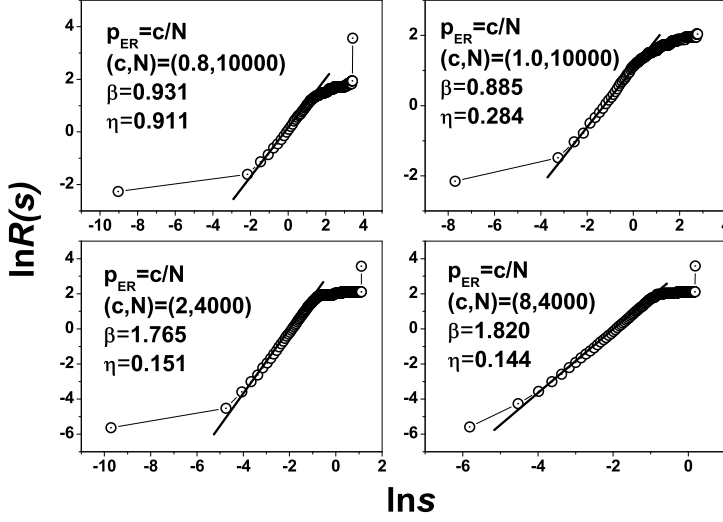


Fig. 2. Determine the values of parameters  $(\beta, \eta)$  for the four Erdos-Renyi networks by means of the relation presented in Eq.12. In the main region we are interested the NNLS distributions obey a Brody form almost exactly. For  $p_{ER} < p_c = \frac{1}{N}$ , we have  $\beta = 0.931 \sim 1.0$ , i.e., the distribution obeys a Poisson form. For  $p_{ER} > p_c$ , the distributions obey a Brody distribution form very near the Wigner one. The errors of the parameters  $(\beta, \eta)$  are less than 0.01.

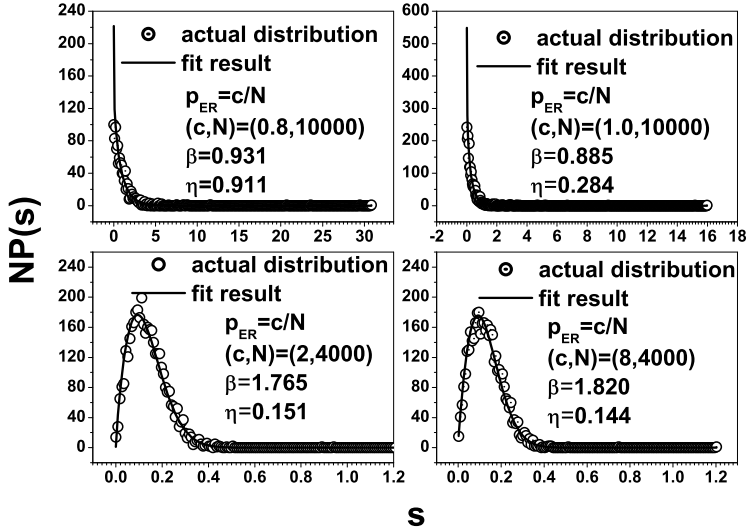


Fig. 3. The NNLS distributions for the four Erdos-Renyi networks. In the main regions we are interested, the theoretical results can fit with the actual ones very well. The errors of the parameters  $(\beta, \eta)$  are less than 0.01.

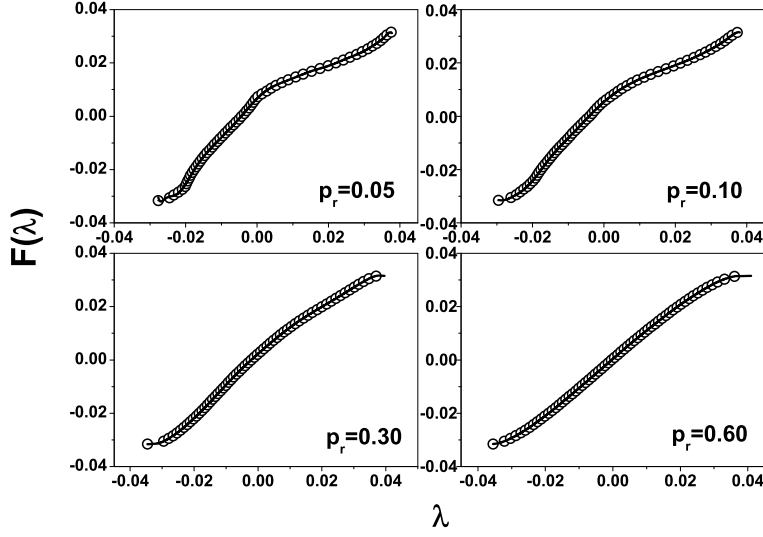


Fig. 4. The cumulative density function of the spectra of four selected WS small-world networks. The circles are the actual values, while the solid lines are fitting results with a 17-ordered polynomial function.

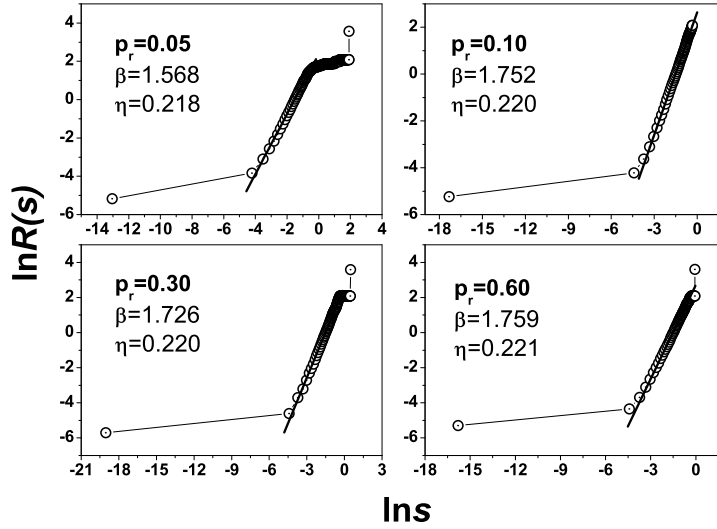


Fig. 5. Determine the values of parameters  $(\beta, \eta)$  for the four selected WS small-world networks by means of the relation presented in Eq.12. In the main region we are interested the NNLS distributions obey a Brody form almost exactly. The errors of the parameters  $(\beta, \eta)$  are less than 0.01.

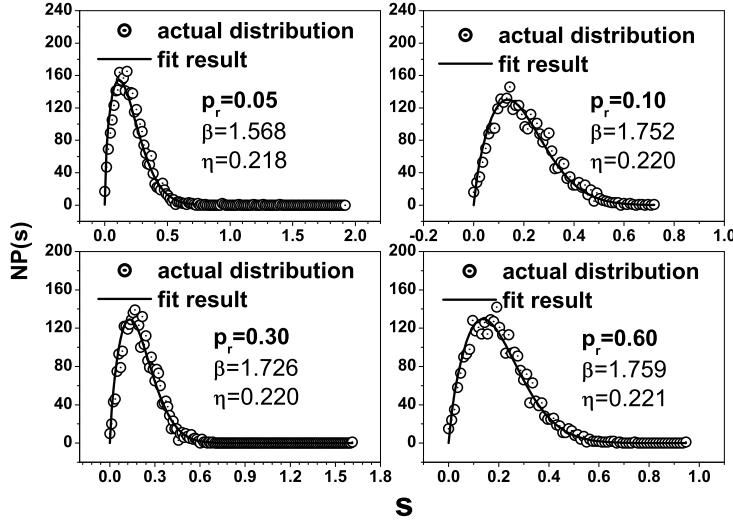


Fig. 6. The NNLS distributions for the four selected WS small-world networks. In the main regions we are interested, the theoretical results can fit with the actual ones very well. The errors of the parameters ( $\beta, \eta$ ) are less than 0.01.

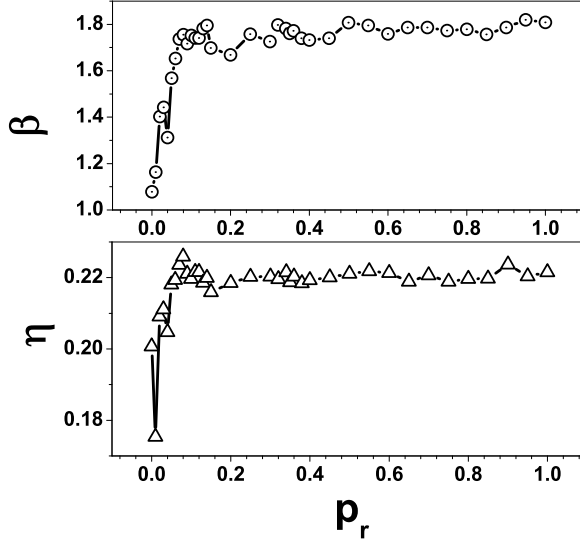


Fig. 7. The parameters ( $\beta, \eta$ ) for all the WS small-world networks constructed in this paper. In the short region  $p_r \in [0.0, 0.1]$ , the value of  $\beta$  increases from 1.0 to 1.75, i.e., the NNLS distribution evolves from a Poisson to a near Wigner form. In the other region  $p_r \in [0.1, 1]$ , the networks behave almost same. Comparison tells us that the Erdos-Renyi networks with  $p_{ER} = \frac{2J}{N}$  ( $J \geq 1$ ) are similar with the WS small-world network with  $p_r = 1$ . The errors of the parameters are less than 0.01.

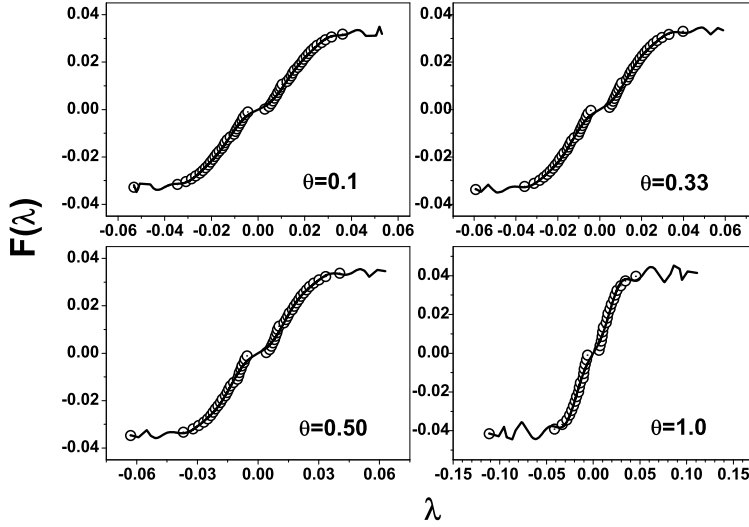


Fig. 8. The cumulative density function of the spectra of four selected GRN networks. The circles are the actual values, while the solid lines are fitting results with a 17-ordered polynomial function.

Brody distribution almost exactly. Fig.7 presents the values of the parameters  $\beta$  and  $\eta$  versus the rewiring probability  $p_r$ . In a short region  $p_r \in [0.0, 0.1]$ , the value of  $\beta$  increases from 1 to 1.75, i.e., the NNLS distribution evolves from a Poisson to a near Wigner form. In the other region  $p_r \in [0.1, 1.0]$  the networks behave almost same. Comparison tells us that the Erdos-Renyi networks with  $p_{ER} = \frac{2J}{N} (J \geq 1)$  are similar with the WS small-world network with  $p_r = 1$ .

The third considered is the growing random networks (GRN) model [30]. Giving several connected seeds, at each step a new node is added and a link to one of the earlier nodes is created. The connection kernel  $A_k$ , defined as the probability a newly introduced node links to a preexisting node with  $k$  degree, determines the structure of this network. A group of GRN networks determined by a special kind of kernel,  $A_k \propto k^\theta (0 \leq \theta \leq 1)$ , are considered in this present paper. For this kind of networks, the degree distributions decrease as a stretched exponential in  $k$ . Setting  $\theta = 1$  we can obtain a scale-free network.

Fig.8 to Fig.10 present some typical results for GRN networks. Fig.11 shows that in a wide range of  $0 \leq \theta \leq 0.8$ , the value of the parameter  $\beta$  oscillates basically around 0.68, i.e., the NNLS distributions deviate significantly from the Poisson form in a way opposite to that of WS small-world networks. In the other region  $p_r \in [0.8, 1.0]$  the value of  $\beta$  decreases rapidly to  $\sim 0.50$ . The values of the parameter  $\eta$  are also presented.

Fig.12 shows the relation between  $\beta$  and  $\eta$ . Each point represents a complex network. The results for the three kinds of networks are all illustrated. The

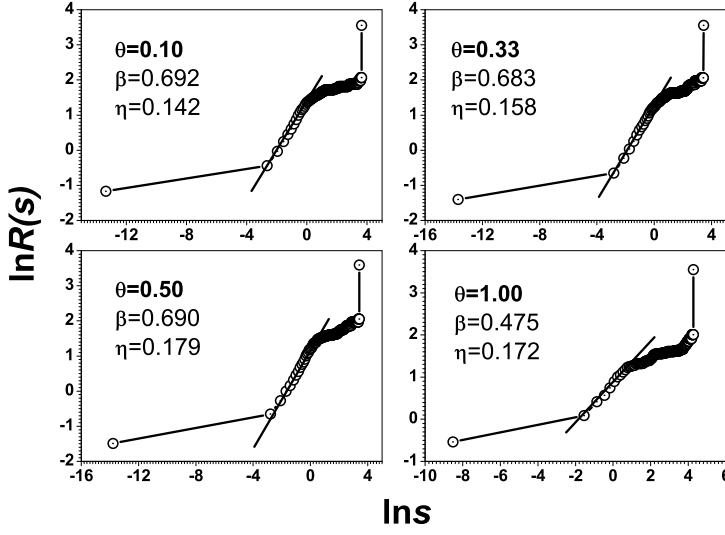


Fig. 9. Determine the values of parameters ( $\beta, \eta$ ) for the four selected GRN networks by means of the relation presented in *Eq.12*. In the main region we are interested the NNLS distributions obey a Brody form almost exactly. The errors of the parameters ( $\beta, \eta$ ) are less than 0.01.

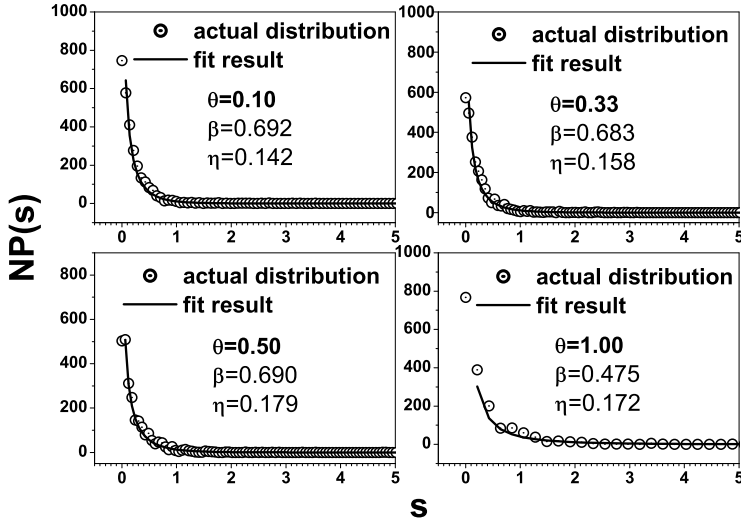


Fig. 10. The NNLS distributions for the four selected GRN networks. In the main regions we are interested, the theoretical results can fit with the actual ones very well. The errors of the parameters ( $\beta, \eta$ ) are less than 0.01.

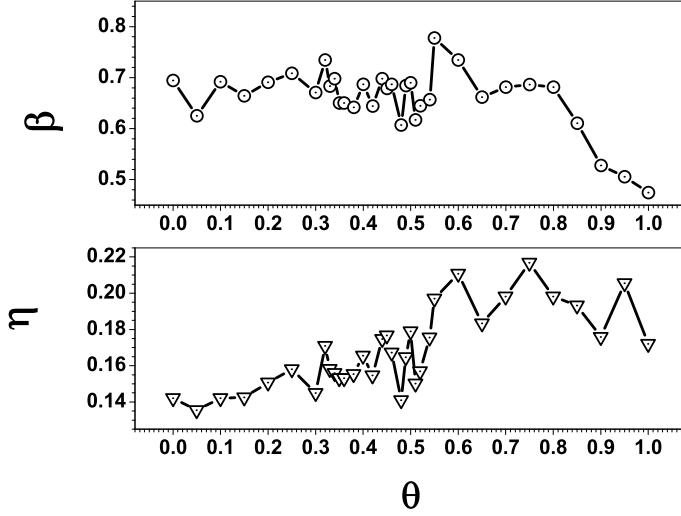


Fig. 11. The parameters  $(\beta, \eta)$  for all the GRN networks constructed in this paper. In a large region  $p_r \in [0.0, 0.8]$ , the value of  $\beta$  oscillates around 0.68, i.e, the NNLS distributions deviate significantly from the Poisson form in a way opposite to that of WS small-world networks. In the other region  $p_r \in [0.8, 1]$ , the value of  $\beta$  decreases rapidly to  $\sim 0.5$ . The errors of the parameters  $(\beta, \eta)$  are less than 0.01.

WS small-world networks and the GRN networks are separated by the Poisson form, i.e.,  $\beta = 1$ , significantly. The Erdos-Renyi networks with  $p_{ER} \leq p_c = \frac{1}{N}$  obey near Poisson distribution, while that with  $p_{ER} > p_c = \frac{1}{N}$  are similar with the almost complete random WS small-world networks ( $p_r \sim 1.0$ ).

## 4 Summary

In summary, based upon the RMT theory we investigate the NNLS distributions for the ER, the WS Small-world and the GRN networks. The Brody form can describe all these distributions in a unified way. The NNLS distributions of the quantum systems of the network of  $N$  coupled identical oscillators tell us that the corresponding classical dynamics on the Erdos-Renyi networks with  $p_{ER} < p_c = \frac{1}{N}$  are in the state of collective order, while that on the Erdos-Renyi networks with  $p_{ER} > p_c = \frac{1}{N}$  in the state of collective chaos. On WS small-world networks, the classical dynamics evolves from collective order to collective chaos rapidly in the region  $p_r \in [0.0, 0.1]$ , and then keeps chaotic up to  $p_r = 1.0$ . For GRN model, contrary to that on the WS small world networks, the classical dynamics are in special states deviate from order significantly in an opposite way.

These dynamical characteristics are determined only by the structures of the

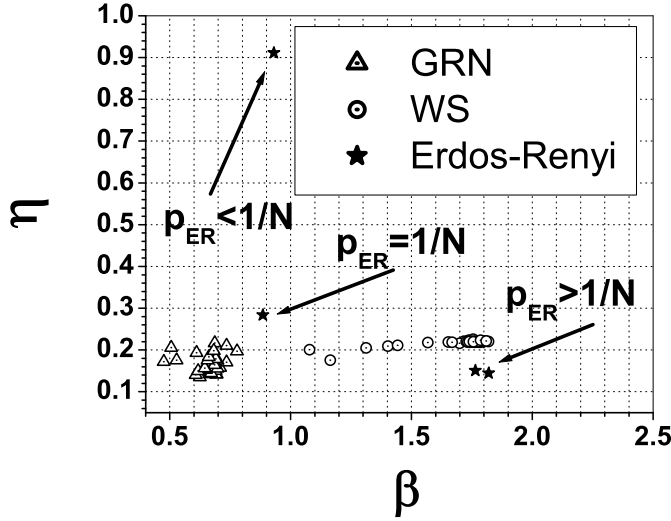


Fig. 12. The relation between the two parameters  $(\beta, \eta)$ . Each point corresponds to a complex network. The results for the three kinds of networks are all illustrated. The WS small-world networks and the GRN networks are separated by the Poisson form, i.e.,  $\beta = 1$ , significantly. The Erdos-Renyi networks with  $p_{ER} < p_c = \frac{1}{N}$  obey near Poisson distribution, while that with  $p_{ER} \geq p_c$  are similar with the almost complete random WS small-world networks ( $p_r \sim 1$ ). The position of a network in this scheme may tell some useful information. The errors of the parameters  $(\beta, \eta)$  are less than 0.01.

considered complex networks. In a very recent paper [31], the authors point out that for some biological networks the NNLS distributions obey the Wigner form. The dynamics on these networks should be in a state of collective chaos. And the removal of nodes may change this dynamical characteristic from collective chaos to collective order. Therefore, constructing a mini network with selected key nodes should be considered carefully in discussing the collective dynamics on a complex network.

Without the aid of the simplified model of dynamics presented in [3,4] we obtain the dynamical characteristics on complex networks. The NNLS distribution can capture directly the relation between the structure of a complex network and the dynamics on it.

It should be pointed out that the collective chaos induced by the structures of complex networks is completely different with the individual chaotic states of the oscillators on the networks. For a network with regular structure, the classical dynamical processes on it should display collective order, even if the coupled identical oscillators on the nodes may be in chaotic states. On the contrary, for a complex network with a complex structure (e.g., a WS small-world structure), the classical dynamical processes on it should display col-

lective chaos, even if the coupled identical oscillators on the nodes may be in order states as harmonic oscillations.

Each network can be measured by a couple values of  $(\beta, \eta)$ . The position of a complex network in  $\beta$  versus  $\eta$  scheme may tell us useful information for classification of real world complex networks.

## 5 Acknowledgements

This work was partially supported by the National Natural Science Foundation of China under Grant No. 70471033, 10472116 and No.70271070. One of the authors (H. Yang) would like to thank Prof. Y. Zhuo, Prof. J. Gu in China Institute of Atomic Energy and Prof. S. Yan in Beijing Normal University for stimulating discussions.

## References

- [1] M. E. J. Newman, SIAM Review **45**, 117(2003).
- [2] F. Liljeros, C. R. Edling, L. A. N. Amaral, H. E. Stanley and Y. Aberg, Nature **411**, 907(2001).
- [3] H. Yang, F. Zhao, Z. Li, W. Zhang and Y. Zhou, Int. J. Mod. Phys. B **18**, 2734(2004).
- [4] B.-Y. Yaneer and I. R. Epstein, Proc. Natl. Acad. Sci. **101** 4341(2004).
- [5] F. Li, T. Long, Y. Lu, Q. Ouyang and C. Tang, Proc. Natl. Acad. Sci. **101**,4781(2004).
- [6] M. Barahona and L. M. Pecora, Phys. Rev. Lett. **89**, 054101(2002).
- [7] T. Zhou, M. Zhao and B. Wang, arXiv.org:cond-mat/0508368.
- [8] M. Zhao, T. Zhou and B. Wang, arXiv.org:cond-mat/0507221.
- [9] S. Jalan, R. E. Amritkar and C. -K. Hu, arXiv.org: nlin.CD/0307037.
- [10] T. Guhr, A. Mueller-Groeling, and H. A. Weidenmueller, Phys. Rep. **299**, 189 (1998).
- [11] M. L. Mehta, *Random Matrices* (Academic Press,Boston, 1991).
- [12] T. A. Brody, J. Flores, J. B. French, P. A. Mello, A. Pandey, and S. S. M. Wong, Rev. Mod. Phys. **53**, 385(1981).

- [13] I. J. Farkas, I. Deranyi, A. -L. Barabasi, and T. Vicsek, Phys. Rev. E **64**, 026704 (2001).
- [14] R. Berkovits and Y. Avishai, Phys. Rev. B **53**, R16125(1996).
- [15] S. N. Dorogovtsev, A. V. Goltsev, J. F. F. Mendes, and A. N. Samukhin, Phys. Rev. E **68**, 046109 (2003).
- [16] M. A. M. de Aguiar and Y. Bar-Yam, Phys. Rev. E **71**, 016106(2005).
- [17] C. Zhu, S. Xiong, Y. Tian, N. Li and K. Jiang, Phys. Rev. Lett. **92**, 218702 (2004).
- [18] H. Yang, F. Zhao, L. Qi and B. Hu, Phys. Rev. E **69**, 066104(2004).
- [19] F. Zhao, H. Yang and B. Wang, arXiv.org: cond-mat/0509012. To be published in Phys Rev. E.
- [20] U. Magnea, arXiv.org: math-ph/0502015.
- [21] K. B. Efetov, arXiv: cond-mat/0502322.
- [22] V. Plerou, P. Gopikrishnan, B. Rosenow, L. A. N. Amaral, T. Guhr and H. E. Stanley, Phys. Rev. E **65**, 066126(2002).
- [23] <http://www.weibull.com/basics/lifedata.htm>
- [24] I. C. Percival, J. Phys. B **6**, L229(1973).
- [25] N. Promphery, J. Phys. B **7**, 1909(1974).
- [26] M. V. Berry and M. Tabor, Proc. Roy. Soc. Lond. A **356**, 375(1977).
- [27] P. Erdos, A. Renyi, Publ. Math. Inst. Hung. Acad. Sci. **5**, 17(1960).
- [28] B. Bollobas, Random Graphs (Academic Press, London, 1985).
- [29] D. J. Watts and S. H. Strogatz, Nature (London) **393**, 440 (1998).
- [30] P. L. Krapivsky, S. Redner, and F. Feyvraz, Phys. Rev. Lett. **85**, 4629 (2000).
- [31] F. Luo, J. Zhong, Y. Yang, R. H. Scheuermann, J. Zhou, arXiv:cond-mat/0503035.